Fast waves during transient flow in an asymmetric channel

Dick Kachuma & Ian Sobey

Oxford University Computing Laboratory
Wolfson Building, Parks Road,
Oxford UK OX1 3QD
dick.kachuma@comlab.ox.ac.uk
ian.sobey@comlab.ox.ac.uk

1. Introduction

The use of stepped channels together with unsteady laminar flow provides a powerful mixing mechanism that is particularly applicable to processes where the fluid contains delicate elements, for example, applications involving mass transfer in blood or in a cell culture. In such channel flows there are parameter regimes where the flow is described by the two-dimensional unsteady Navier–Stokes equations. In [1], it was shown both experimentally and numerically that a standing wave of separated regions develops behind a channel step during oscillatory flow and the resulting flow was called a vortex wave. Included in the experimental observations were vortex waves of extreme longitudinal extent and it was conjectured that the wave formed was, under the correct parameter conditions, virtually undamped in the streamwise direction. We have undertaken calculations in a slightly different parameter region and find that a sequence of two events occurs: one is the formation of a vortex wave of finite extent (typically 3-5 vortices alternating on the two walls behind the step), the second is a subsequent rapidly propagating wave of regular but slightly smaller vortices. The speed of propagation of this second wave is such that its resolution would have been beyond that of the apparatus used in [1]. In describing these waves we shall refer to the vortex wave as a V-wave and the second wave as a KH-wave. An example of the waves is illustrated in figure 1 where streamlines of a flow are shown for one time in a cycle.

V-wave   KH-wave
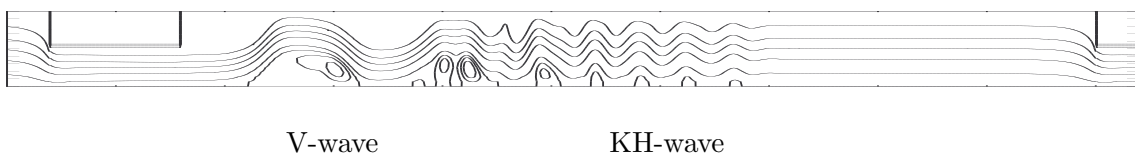
Figure 1: Instantaneous streamlines

In order to understand the genesis of KH-waves we have undertaken a study of starting flows where the fluid is accelerated from rest to either steady channel flux or a flux with an oscillatory component. The results presented below are for pure oscillatory flow. We test two hypotheses: one that the KH-wave results from the evolution of an inviscid rotational core flow that is described by an evolutionary linearised Kortweg-de Vries (KdV) equation. That this might be a plausible hypothesis comes from results in [3] which show the evolution of waves in solutions of an evolutionary KdV equation. The second hypothesis is that the KH-wave results from an Orr-Sommerfeld type instability of nearly parallel but non-Poiseuille like flow. This has lead us to study stability of a base flow $u_0(y) = (3/2)(1 - \sigma y)(1 - y^2)$, $-1 \leq y \leq 1$, where $\sigma = 0$ is Poiseuille flow and $\sigma > 1$ indicates reverse flow near one wall.

The paper is divided into four sections. We briefly describe the numerical solution of the unsteady Navier–Stokes equations and illustrate the development of a KH-wave. We integrate

velocities in time to obtain particle paths and use these to help interpret the development of the flows. We describe solutions of an evolutionary linearised KdV equation and their interpretation. We consider solutions of an Orr-Sommerfeld equation for a parallel flow with a reverse flow region and investigate unstable solutions to that system.

While much work is still in progress, the results we have indicate that it is unlikely that the KH-wave is the result of evolution of an inviscid rotational core flow and instead, that it is more likely the result of a linear instability mechanism described by an Orr–Sommerfeld equation but with growth rates that are orders of magnitude greater than those for disturbances to symmetric Poiseuille flow and with instability occuring at relatively low Reynolds number. The complexity of unsteady flows calculated from the full Navier–Stokes equations is remarkable and it is likely that flows in other parameter regimes may be dominated by entirely different mechanisms.

2. Numerical solution of the unsteady Navier–Stokes equations

We consider incompressible viscous flow in a two dimensional periodic channel with inlet width h and a sudden expansion to a width $2h$. We take h as a length scale, (x, y) as non-dimensional coordinates with x as the channel streamwise direction and fluid kinematic viscosity ν. We let L denote the non-dimensional length of one section of the channel and L_h the non-dimensional length of the expansion. We show such a channel in figure 2 which has $L = 96$ and $L_h = 84$. It is such large values of L and L_h that allow enough room for the fast waves to develop.
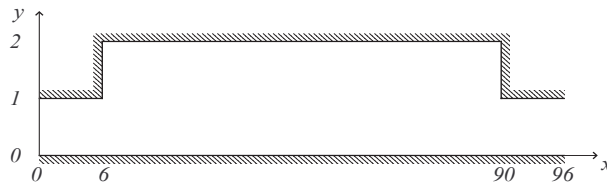
Figure 2: Schematic of two-dimensional channel

If the flux per unit width of channel is $Q(\hat{t}/T_s)$ where $\hat{t}$ is dimensional time and T_s a characteristic timescale imposed by the oscillation, define non-dimensional time $t = \hat{t}/T_s$. Assuming that the peak flux is $2Q_{max}$ so that for some $q(t)$, $Q = 2Q_{max}q(t)$, define a velocity scale $U_0 = Q_{max}/h$, a Reynolds number Re and a Strouhal number St as

$$\mathrm{R}e = \frac{U_0 h}{\nu} = \frac{Q_{max}}{\nu}, \qquad \mathrm{S}t = \frac{h}{U_0 T_s} = \frac{h^2}{Q_{max} T_s}.$$

For oscillatory flow we have $q(t) = \sin 2\pi t$, while if there is a mean flow $\bar{Q}$ (typically < 1), the ratio of mean forward flux to peak forward flux, a more general form of $q(t)$ is $q(t) = \bar{Q} + (1 - \bar{Q}) \sin 2\pi t$ with $\bar{Q} = 1$ implying steady flow.

Since the flow field is two-dimensional we use the streamfunction-vorticity formulation, so that the velocities in the (x, y) directions are $\mathbf{u} = (u, v)$, respectively. We define a streamfunction, ψ, and vorticity, ω, by

$$u = \psi_y, \quad v = -\psi_x, \quad \omega = -u_y + v_x = -\nabla^2 \psi. \tag{1}$$

The Navier–Stokes momentum equations reduce to

$$\mathrm{S}t \frac{\partial \omega}{\partial t} + (\mathbf{u} \cdot \nabla)\omega = \frac{1}{\mathrm{R}e} \nabla^2 \omega. \tag{2}$$

The boundary conditions are $\psi = -q(t)$ on the lower wall, $\psi = q(t)$ on the upper wall, and $\nabla \psi \cdot \mathbf{n} = 0$ on both walls, where $\mathbf{n}$ is normal to the walls. We impose a periodicity condition on
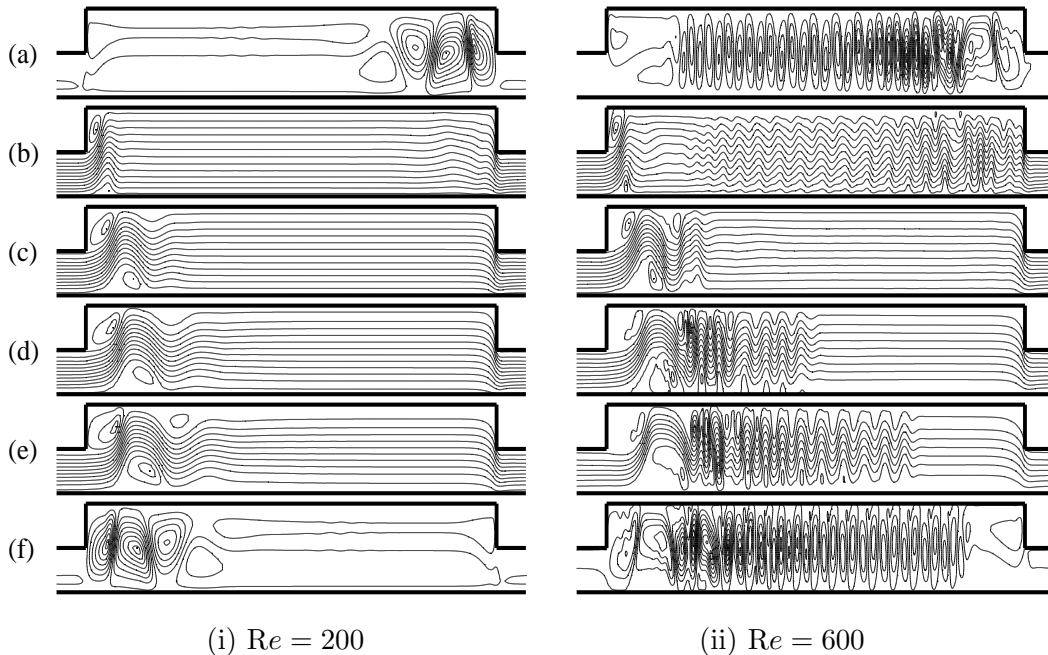
(i) Re = 200   (ii) Re = 600

Figure 3: Instantaneous streamlines showing the development of a vortex wave and subsequent KH-waves. The flow is at St = 0.005 and Re = 200 (i) and Re = 600 (ii) at times t = 2.0 (a), t = 2.1 (b), t = 2.2 (c), t = 2.3 (d), t = 2.4 (e) and t = 2.5 (f). Note that the channel spect ratio is highly distorted with length L = 96 and maximum width 2.

both ψ and ω in the streamwise direction,

$$\psi(x, y, t) = \psi(x + L, y, t), \qquad \omega(x, y, t) = \omega(x + L, y, t).$$

The equations are integrated in time by using a semi-implicit Crank–Nicolson method with standard central differences used for spatial derivatives.

We show in figure 3, the development of vortex waves and the fast waves by plotting the streamlines of the computed fluid flow for Reynolds numbers 200 (i) and 600 (ii) and Strouhal number St = 0.005 over half a period of oscillation. At t = 2.0 (a), the vortices from the preceding half cycle are still present in the channel. As the flow is accelerated to t = 2.1 (b), these effects are eroded and at t = 2.2 (c), long wavelength vortex waves, characterised by 3 or 4 counter-rotating vortices are seen to develop. When the flow starts to decelerate at t = 2.3, (d) the flow at Re = 600 starts to shed shorter wavelength fast-moving waves which travel far downstream (e). The flow at Re = 200 however, does not possess this structure and only develops the long wavelength vortex waves. At t = 2.5, (f) the flux returns to zero and the flow is a reflection of that at t = 2.0 (a). In subsequent half cycles, the patterns reverse and the sequence of vortex wave formation and fast wave shedding repeats. In the case Re = 600, St = 0.005, the Navier–Stokes solutions suggest that the wavelength of the KH-wave is 3-5 non-dimensional units and the frequency near 22 times that of the imposed oscillation.

3. Particle paths

In this section we investigate the movement of particles in oscillatory flow in a channel. The time dependent solutions of the Navier–Stokes equations developed in the preceding section, will be used to trace the trajectories of a cloud of particles which is initially uniformly distributed in one section of the periodic channel. We denote by $\left(x^{(n)}, y^{(n)}\right)$ the position of particle n and hence the equations of motion associated with the particle are

$$\text{S}t\, x_t^{(n)} = u(x^{(n)}, y^{(n)}, t), \qquad \text{S}t\, y_t^{(n)} = v(x^{(n)}, y^{(n)}, t), \tag{3}$$

3

where u and v are the time dependent velocity fields of the fluid given by the solution of the Navier–Stokes equations. This assumes that the particles move in the fluid without affecting the underlying flow and that they move as fluid particles. We denote by N_p the total number of particles and we have performed the computations for three values of N_p, $N_p = 2880$, $N_p = 11520$ and $N_p = 46080$. Our calculations show that the results obtained to not vary significantly with the number of particles.
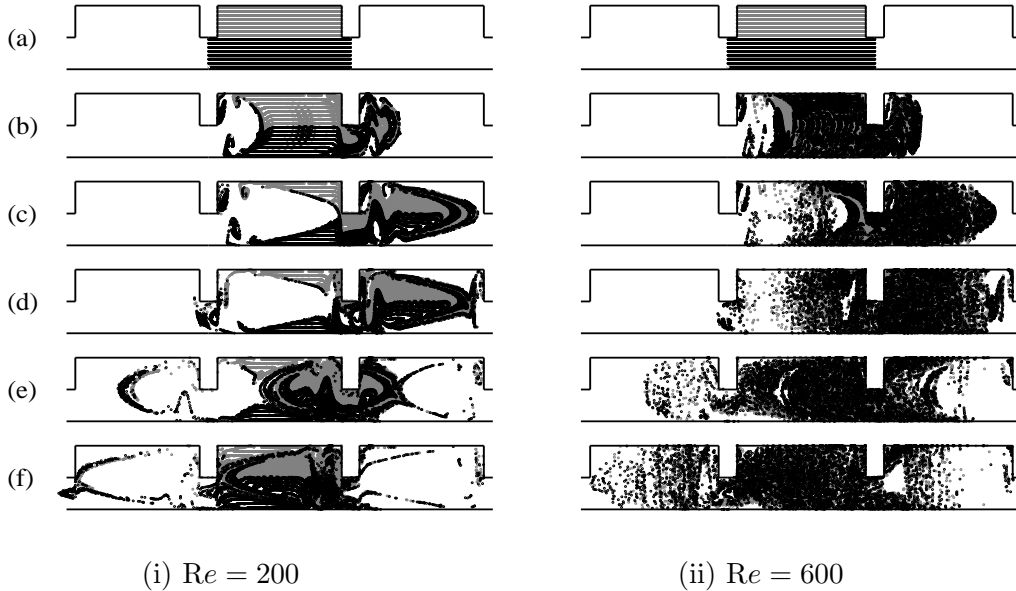
| (i) R$e = 200$ | (ii) R$e = 600$ |

Figure 4: Particle trajectories for flows at R$e = 200$ (i) and R$e = 600$ (ii) at Strouhal number S$t = 0.005$. The particles are initially uniformly distributed at $t = 1$ (a) and are subsequently shown at $t = 1.1$ (b), $t = 1.2$ (c), $t = 1.3$ (d), and $t = 1.4$ (e).

We show in figure 4, the motion on particles. The figure shows a scatter plot of the positions of the particles at different times during one cycle of oscillation. The figure shows particles for the Reynolds numbers 200 (i) and 600 (ii) and Strouhal number S$t = 0.005$ with the particles are coloured black or gray depending on the half of the channel in which they are initially positioned. The diagram illustrates the increase in transverse mixing at the higher Reynolds number.

As a measure of the scatter of the particles we compute the variance σ_x^2 of the longitudinal position

$$\sigma_x^2(t) = \frac{1}{N_p - 1} \sum_{i=1}^{N_p} (x_i(t) - \bar{x}(t))^2,$$

where $\bar{x}(t) = \frac{1}{N_p} \sum_{i=1}^{N_p} x_i(t)$ is the mean of the distribution. We can therefore approximate the instantaneous dispersion coefficient [4] $D(t) = \frac{1}{2} \frac{d\sigma_x^2}{dt}$ and integrating this over one cycle of oscillation gives a cycle dispersion coefficient

$$K = \int_{\text{cycle}} D(t) dt = \frac{1}{2} \Delta \sigma_x^2 \Big|_{\text{cycle}}$$

Figure 5 (i) shows the instantaneous variance σ_x^2 of the longitudinal position at S$t = 0.005$ for R$e = 200$ and R$e = 600$. This shows an overall linear growth of the variance over time with oscillations at the same frequency as the underlying flow. The dipersion coefficient over one cycle K is shown in figure 5 (ii) as a function of the Reynolds number at S$t = 0.005$. This shows that the dispersion increases with Re until R$e > 500$ when it begins to decline thus revealing that a rapid increase in mixing occurs when the KH-wave forms.

4
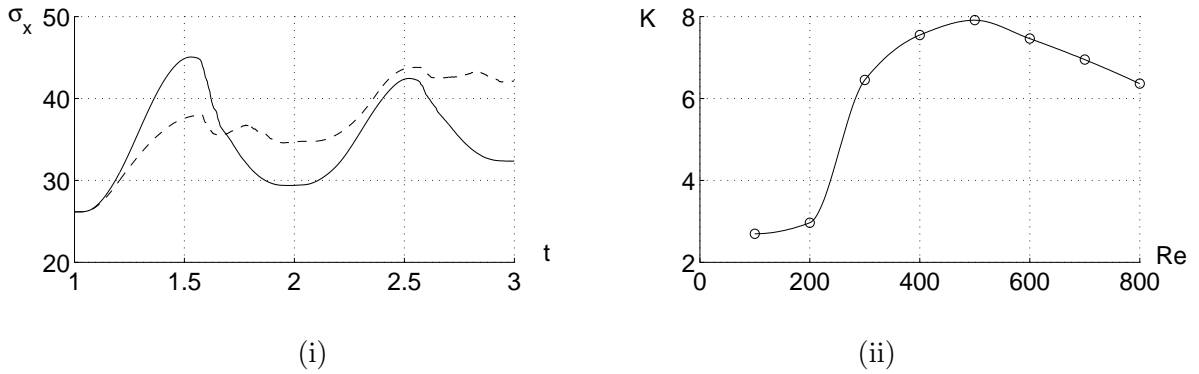
Figure 5: (i) Instantaneous variance $\sigma_x^2(t)$ of the longitudinal position of particles at $St = 0.005$ and $Re = 200$ (solid) and $Re = 600$ (dashed). (ii) Cycle dispersion coefficient K as a function of Re at $St = 0.005$ computed over the interval $t \in [1, 2]$.

4. Inviscid Theory

We develop, in this section, an inviscid theory for the generation of the vortex wave. The work described here follows closely, the theory developed by [2] and [3]. We consider a smooth-walled channel in which the size of indentations is small compared to the width of the channel. We suppose that the lower wall of the channel is fixed at $y = -1$ and that the upper wall is defined by $y = 1 + \epsilon F(x)$ where $\epsilon \ll 1$ and F is a smooth function. A long wavelength approximation is made for the vortex wave and we introduce $\lambda \gg 1$ as a streamwise lengthscale. With this lengthscale the Navier–Stokes equations are transformed so that the streamwise momentum equation is

$$\lambda St u_t + u u_x + v u_y = -p_x + \lambda Re^{-1}(u_{xx} + \lambda^{-2} u_{yy}).$$

We assume a long wavelength approximations [1, 3]

$$u = U_0(y,t) + \epsilon A(x,t) U_{0y}(y,t) + \mathcal{O}(\epsilon^2), \qquad p = P_0(x,t) + \epsilon^2 P(x,t) + \epsilon^2 \rho A_{xx} \int_{-1}^{y} U_0^2 \mathrm{d}y + \mathcal{O}(\epsilon^3),$$

where $A(x,t)$ is as yet an unknown function that indicates the displacement of the centre streamlines. Substituting these expansions into the flow equations and imposing kinematic boundary conditions of zero normal velocity at the walls, we get a linearised KdV equation for the streamline displacement A given by [3]

$$(\gamma A)_t - \beta A_{xxx} = -\varepsilon \gamma^2 (F F_x + F A_x + F_x A), \tag{4}$$

with $\gamma(t) = U_{0y}(-1, t)$ being the lower wall shear and $\beta(t) = \int_{-1}^{1} U_0^2(y,t) \mathrm{d}y$.

The unperturbed flow upstream is taken to be unsteady Poiseuille-like flow given by $u = U_0(y,t)$, $v = 0$ and $p = P_0(x,t) = \lambda Re^{-1} x p_0(t)$ satisfying

$$Re St\, U_{0t} = -p_0(t) + U_{0yy}$$

with the boundary conditions $U_0(\pm 1, t) = 0$ and the flux condition $\int_{-1}^{+1} U_0(y,t) \mathrm{d}y = 2q(t)$. Here p_0 is an unknown unsteady pressure gradient and is determined to satisfy the flux condition. This equation is solved using a Chebyshev collocation method with Clenshaw-Curtis quadrature used to approximate the flux conditions (see for example [5]).

With reference to figure 2 we solve (4) with the boundary function

$$F(x) = 0.5 \left\{ \tanh[\alpha(x - 6)] - \tanh[\alpha(x - 90)] \right\},$$

5

which approaches the desired sudden expansion as $\alpha \to \infty$. We use exponential time stepping with periodic Fourier spectral discretisation for spatial derivatives as described in [6]. We solve the equation for x in the interval $[0, 128]$ which is longer than the channel used in the numerical simulations but reduces the effect of the downstream boundary.
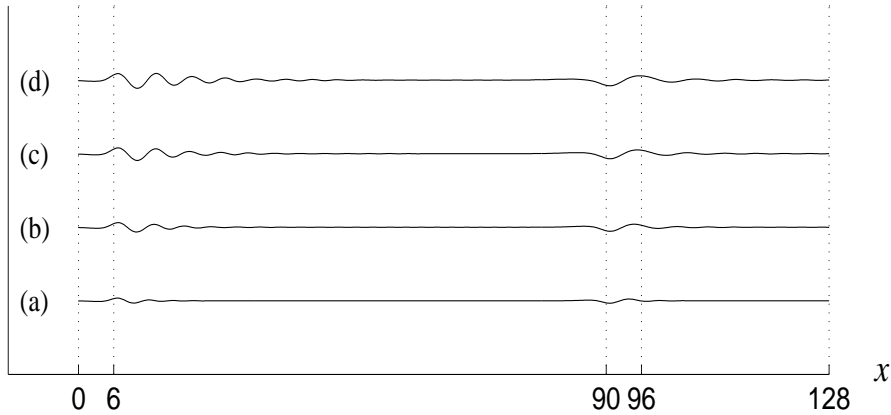
Figure 6: Displacement of centre streamlines $A(x, t)$ given by the solution of (4). The plot of A is given at $t = 1$ (a), $t = 2$ (b), $t = 3$ (c) and $t = 4$ (d).

Figure 6 shows the streamline displacement A as a function of x at the different times and reveals that a wave develops at the expansion and is propagated downstream. There is another smaller wave that develops at the point where the channel width returns to 1. The speed at which these waves propagate is of order 1 and small compared to KH-waves which have speeds of order $\mathrm{S}t^{-1}$ calculated from solutions of the Navier–Stokes equations. The waves computed from the KdV equation have wavelengths that are in the regime of the vortex waves that develops before the flow begins to shed KH-waves.

5. Linear Stability Theory

In the long channel flows we are considering, there are significant regions of almost parallel flow so it is natural to consider whether the genesis of the KH-wave can be explained by considering stability of a parallel flow. There is a substantial classical theory that considers linear disturbances to a parallel flow although its application to symmetric channel flow has in recent times been deprecated because predicted growth rates when the underlying flow is unstable are so small that the time or travel distance needed for a disturbance to develop are unrealistically long. The model we examine here takes the unperturbed flow to be

$$u_0(y) = \frac{3}{2}(1 - \sigma y)(1 - y^2), \quad -1 \le y \le 1, \tag{5}$$

with wall shear at $y = 1$ given by $u'(1) = 3(\sigma - 1)$ so that the profile can represent reverse flow near one wall when $\sigma > 1$. The choice of profile is significant because it preserves the flux through a channel as σ is varied. Example profiles are shown in figure 7.

When the parallel flow, (5), is perturbed as

$$u \sim u_0(y) + \mathrm{e}^{\mathrm{i}k(x-ct)}\psi'(y), \quad v \sim -\mathrm{i}k\mathrm{e}^{\mathrm{i}k(x-ct)}\psi(y), \tag{6}$$

the function $\psi(y)$ of the perturbation satisfies an Orr-Sommerfeld equation

$$(u_o - c\mathrm{S}t)D^2\psi - u_0''\psi = \frac{1}{\mathrm{i}k\mathrm{R}e}D^4\psi, \tag{7}$$

6
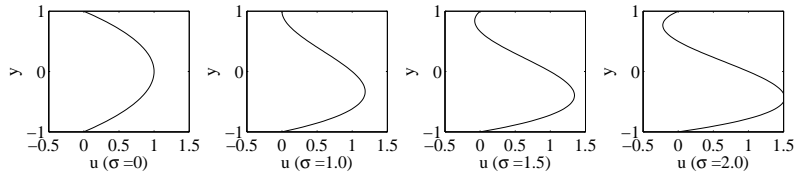
Figure 7: Example parallel flow velocity profiles for $\sigma = 0, 1.0, 1.5, 2.0$

where $D^2 = \mathrm{d}^2/\mathrm{d}y^2 - k^2$ and $\psi(\pm 1) = \psi'(\pm 1) = 0$. It is well known that the symmetric case, $\sigma = 0$, becomes unstable to small disturbances ($c_i = Im(c) > 0$) at a critical value $\mathrm{R}e \approx 3848$ (because of scaling in (5), value is 2/3 of 5772) but also that at Reynolds numbers above this critical value, the amplification of disturbances is minute, for example at $\mathrm{R}e = 4000$, the maximum amplification per cycle of the disturbance is 1.0156, implying near 148 cycles for a disturbance to grow by one order of magnitude. However, it is not generally appreciated that the symmetric case is in a sense an anomalous case, and that when the parallel flow is asymmetric, the predictions of linear stability theory are much different. In figure 8 the critical reynolds number for loss of stability is shown as the asymmetry parameter σ is varied. For small values of σ the critical Reynolds number increases but for values where reverse flow exists at one wall, the critical Reynolds number decreases to less than 100.
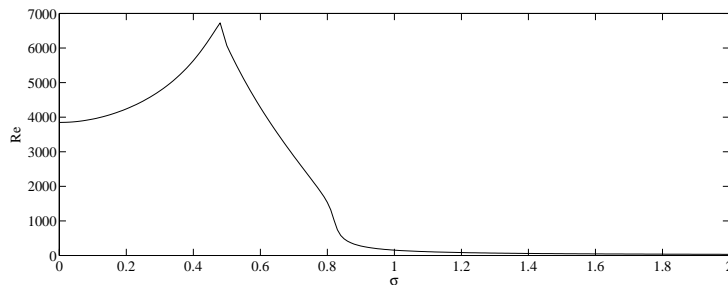
Figure 8: Critical Reynolds number for instability as the asymmetry parameter σ is varied.

In order to compare the predictions to computed Navier–Stokes flows it is useful to observe that the disturbance is essentially like

$$\mathrm{e}^{kc_i t}\mathrm{e}^{\mathrm{i}k(x - c_r t)},$$

so that the wavelength of a disturbance is $\lambda = 2\pi/k$, the frequency of a disturbance is $\Omega = kc_r/2\pi\mathrm{S}t$ and the amplification per cycle, denoted ζ, is $\zeta = \exp(2\pi c_i/c_r)$. At $\mathrm{R}e = 600$ and $\sigma = 1.5$, the maximum growth per cycle is 3 and an order of magnitude growth occurs in only a few cycles. The growth rate is even larger for higher values of σ, see figure 9 so that near $\sigma = 2$, an order of magnitude growth occurs in only one cycle. Furthermore, the frequency of disturbances is very high, for example in a periodic flow with $\mathrm{R}e = 600$, $\mathrm{S}t = 0.005$, $\sigma = 2$, Orr–Sommerfeld solutions predict the frequency of a disturbance to be around 19 times the imposed oscillatory frequency and a non-dimensional wavelength near 6.

6.   Discussion

The KH-wave illustrated above is, we believe, a previously unreported flow pattern associated with unsteady flow through channels. Our work so far tends to exclude modelling the wave as the result of a long wave-length disturbance to a rotational core flow. Our preliminary results when modelling the wave using linear stability theory show some correspondence but are not conclusive. Computations of the Navier–Stokes equations at $\mathrm{R}e = 600$, $\mathrm{S}t = 0.005$

7
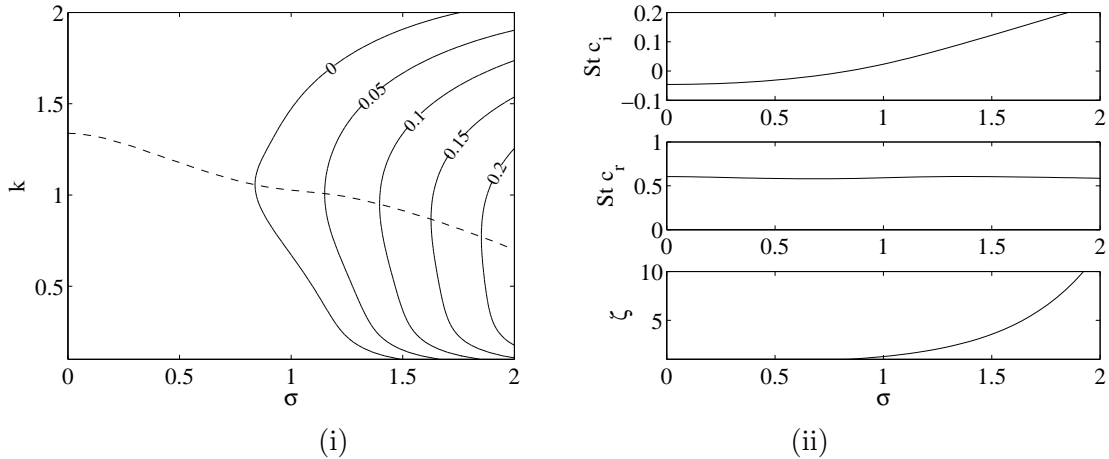
Figure 9: (i) Contours of $\mathrm{S}tc_i$ as σ and k are varied. The flow is unstable where $c_i > 0$. The dashed line shows values of wavenumber k where c_i is maximum for fixed σ. (ii) Real and Imaginary parts of maximum eigenvalue $\mathrm{S}tc$ and corresponding growth per cycle, ζ, for $\mathrm{R}e = 600$ as σ is varied.

indicate the KH-wave has approximate wavelength 3-5 and frequency around 22 the imposed frequency whereas the Orr-Sommerfeld prediction for $\sigma = 2$ is wavelength 6 and frequency multiple 19. Of course the Navier–Stokes solutions are for an evolving flow so perhaps this degree of correspondence is the best that will emerge. In addition, studying the distribution of vorticity for the Navier–Stokes solutions suggest that the emergence of this fast travelling wave also follows a Kelvin-Helmholz roll instability of the vorticity layer between vortices near a wall and the main flow but there are still questions as to why such an instability occurs near specific vortices and not near all.

Acknowledgement

References

[1] I. J. Sobey, "Observation of waves during oscillatory channel flow" *Journal of Fluid Mechanics*, **151**, 395–426 (1985).

[2] O. R. Tutty and T. J. Pedley, "Oscillatory flow in a stepped channel", *Journal of Fluid Mechanics*, **247**, 197–204 (1993).

[3] O. R. Tutty and T. J. Pedley, "Unsteady flow in a nonuniform channel: A model for wave generation", *Physics of Fluids*, **6**, 199–208 (1994).

[4] T.-H. Hwu and I. J. Sobey and B. J. Bellhouse, "Observation of concentration dispersion in unsteady defelected flows", *Chemical Engineering Science*, **51**, 3373–3390 (1996).

[5] L. N. Trefethen, *Spectral Methods in MATLAB*, SIAM, (2000).

[6] A.-K. Kassam and L. N. Trefethen, "Fourth-order time-stepping for stiff pdes", *SIAM Journal of Scientific Computing*, **481**, 1214–1233 (2003).